CLUSTERS OF CYCLONES ENCIRCLING JUPITER'S POLES

Adriani A. (1)*, Mura A. (1), Orton G. (2), Hansen C. (3), Altieri F. (1), Moriconi M.L. (4), Rogers J. (5), Eichstädt G. (6), Momary T. (2), Ingersoll A. (7), Filacchione G. (1), Sindoni G. (1), Tabataba-Vakili F. (2), Dinelli B.M. (4), Fabiano F. (4,8), Bolton S.J. (9), Connerney J.E.P. (10), Atreya S.K. (11), Lunine J.I. (12), Tosi F. (1), Migliorini A. (1), Grassi D. (1), Piccioni G. (1), Noschese R. (1), Cicchetti A. (1), Plainaki C. (13), Olivieri A. (13), M.E. O'Neill (15), Turrini D. (1,14), Stefani S. (1), Sordini R. (1) and Amoroso M. (13)

(1) INAF-Istituto di Astrofisica e Planetologia Spaziali, Roma, Italy
(2) Jet Propulsion Laboratory, California Institute of Technology, Pasadena, California, USA
(3) Planetary Science Institute, Tucson, Arizona, USA
(4) CNR-Istituto di Scienze dell'Atmosfera e del Clima, Bologna e Roma, Italy
(5) British Astronomical Association, London, UK
(6) Independent Scholar, Stuttgart, Germany
(7) California Institute of Technology, Pasadena, California, USA
(8) Dipartimento di Fisica e Astronomia, Università di Bologna
(9) Southwest Research Institute, San Antonio, Texas, USA
(10) NASA Goddard Space Flight Center, Greenbelt, Maryland, USA
(11) University of Michigan, Ann Arbor, Michigan, USA
(12) Cornell University, Ithaca, New York, USA
(13) Agenzia Spaziale Italiana, Roma, Italy
(14) Departamento de Fisica, Universidad de Atacama, Copayapu 485, Copiapò, Chile
(15) Dept. of the Geophysical Sciences University of Chicago, Chicago, USA

Corresponding author: Alberto Adriani (alberto.adriani@iaps.inaf.it)

The familiar axisymmetric zones and belts that characterize Jupiter's weather system at low- to mid-latitudes give way to pervasive cyclonic activity at higher latitudes[1]. Two-dimensional turbulence in combination with the Coriolis β-effect (i.e. the large meridionally-varying Coriolis force on the giant planets) produces alternating zonal flows[2]. At a critical ratio between the Rhines length scale L_R and the Rossby deformation scale L_D, when $L_D/L_R<1$, the zonal flow is expected to cease, which suggests a transition between equatorial jets and polar turbulence on Jupiter[3,4]. Simulations with shallow-water models support this transition by producing both alternating flows near the equator and circumpolar cyclones near the poles[5,6,7,8,9]. Jovian polar regions are not visible from Earth due to Jupiter's low axial tilt, and were poorly characterized by previous missions because their trajectories did not venture far from the jovigraphic equatorial plane. Here we **report that visible and infrared images obtained from above each pole by the Juno spacecraft during its first five orbits reveal persistent polygonal patterns of large cyclones, observed by the Juno spacecraft during its first five orbits. In the North, eight circumpolar cyclones**

are observed about a single polar cyclone; in the South, the polar cyclone is encircled by five circumpolar cyclones. Cyclonic circulation is established via time-lapse imagery obtained over intervals ranging from 20 minutes to 4 hours. Although migration of cyclones toward the pole might be expected as a consequence of the Coriolis β-drift, where cyclonic vortices naturally drift toward the rotational pole, the configuration of the cyclones is without precedent on other planets including Saturn's polar hexagonal features. The manner by which they persist without merging and the process by which they evolve to their current configuration are unknown.

NASA's Juno spacecraft[10,11] has been operating in a 53-day polar orbit of Jupiter since 5 July 2016. The spacecraft has passed close to the planet six times as of this writing, on five of which instruments on board were able to sound the planet and observe myriad interesting atmospheric structures[12,13,14,15]. The Juno spacecraft is in a high-inclination orbit with perijove approximately 4000 km above the cloud tops, passing from pole to equator to pole in about two hours. From their unique vantage point above the poles, JIRAM[16,17] (Jupiter InfraRed Auroral Mapper) and JunoCam[18], onboard Juno, obtained unprecedented views of Jupiter's polar regions. JIRAM is an infrared imager suitable for atmospheric mapping and JunoCam is a pushframe visible camera. Jupiter flybys took place at perijove 1 on 28 Aug. 2016, perijove 3 on 11 Dec. 2016, perijove 4 on 2 Feb. 2018, and perijove on 27 Mar. 2017 (no remote-sensing observations were collected during perijove 2).

The atmospheric structure in Jupiter's polar regions is very different from the well-known axisymmetric banding of alternating belts and zones at lower latitudes. The polar turbulence predicted by models is consistent with initial close-up observations in the visible[15]. Cyclones, as opposed to anticyclones, were expected in the polar regions as a result of the β-effect[9,19,20]. What was unexpected is their stable appearance, close clustering and symmetry around each of the poles.

The Northern Polar Cyclone (NPC, Fig. 1) has a diameter of approximately 4,000 km (on the JIRAM infrared images). It is offset relative to the geographic North Pole by about 0.5° and is surrounded by eight circumpolar cyclones (CPCs) in a double-squared geometrical pattern (Figs. 1, 2). Counting alternating cyclones, four are centred at ~ 83.3°N while the other four at ~ 82.5°N. The square formed by the latter cyclones form is shifted with respect to the former by 45° longitude, forming a "ditetragonal" shape, making the variation of angular distances between the centre of one cyclone to the next from 43° to 47°. All cyclones have similar dimensions with diameters ranging from 4,000 to 4,600 km. Spiral arms are prominent in their outer regions, but tend to disappear in their inner regions except in the NPC itself. These arms define an additional sphere of influence beyond the "cores" in which co-rotating material can be found. The four cyclones furthest from the NPC have broad cloud-covered inner regions with sharp oblate boundaries. The four cyclones interspersed between them have more diverse and irregular inner regions, with very small-scale cloud textures; some of them appear chaotic and turbulent.

The Southern Polar Cyclone (SPC, Figs. 1, 2) is surrounded by five large cyclones in a quasi-pentagonal pattern. They are of similar size, but generally bigger than the northern CPCs with diameters ranging between 5,600 km and 7,000 km. The southern cyclones present a range of morphologies, although the differences are much less distinct than in the north. In particular,

some of them display a quasi-laminar circulation: the SPC and two adjacent CPCs have cloud spirals converging to the center, while the other three CPCs appear to be significantly turbulent along their spiral cloud branches. The SPC has an offset of about 1-2° relative to the geographical South Pole position and the angular distance between two adjacent CPCs is not as regular as in the north, it: can vary from 65° to 80° relative to the centre of rotation of the SPC.

Figures 1 and 2 show the correspondence between the features in JIRAM maps and in JunoCam images. Regions that are relatively bright in the JunoCam images are cool in the JIRAM thermal infrared images and regions that are relatively dark in the visible are warm. As the JIRAM thermal radiance in the ~5-μm M-band is primarily governed by cloud opacity, regions that appear warm can be interpreted as relatively clear of clouds, allowing radiance from deeper, warmer regions to be detected and regions that appear cold are cloudier. Thus, the visibly bright discrete features in the JunoCam images in Figs. 1 and 2 correspond to high-altitude clouds, while the general darker background corresponds to a deeper cloud deck. This corresponds to a general qualitative result from JunoCam observations made in PJ1, that visually bright regions corresponded to regions also relatively bright in the 890-nm band that is sensitive to absorption by methane gas, implying high-altitude clouds in those regions[14]. Figure 3, with the highest resolution maps of the polar regions, gives a detailed view of the polar morphologies showing JIRAM images corresponding to brightness temperatures in the 190 – 260 K range.

In most cases, the cyclones are essentially in contact if one includes the spiral arms that extend beyond the core. In some cases, a single cloud streak connects the outer spiral arms of adjacent cyclones and can be seen to be continuously stretched. The SPC is in contact with the five CPCs around it. In contrast, the PJ4 JIRAM animation reveals a chaotic zone between the NPC and the eight surrounding CPCs, within which there is a largely continuous westward (clockwise) flow at ~86ºN; poleward of this, the eastward (counter clockwise) flow of the NPC begins. This chaotic zone appears to contain turbulent small-scale cloud textures and a few small anticyclonic vortices. The largest of these, located between the NPC and the CPCs, may be identical to a similar anticyclonic vortex at PJ5, having moved westward by 31º longitude in Juno's 53-day orbital period. JIRAM data acquired during PJ4 cover a time span of about 2 hours at each pole, enabling monitoring of the movements of the clouds and other structures that are evident within each cyclone, which in turn permits the identification of cyclonic and anticyclonic zones. The velocity field inside each cyclone is not straightforward to evaluate from these data, both because the pointing inaccuracy of JIRAM is not negligible when dealing with fine scale structures inside cyclones, and because details whose movement is visible are not scattered uniformly. Table 1 provides a summary of preliminary JIRAM measurements of rotational speeds of individual CPCs at 1,500 km from their respective centres.

The changes occurring in the polar polygons can be seen by the JIRAM observations with a time lapse about 53 terrestrial days between PJ4 and PJ5 (Extended Data Figure 1). By this analysis, the northern eight CPCs appear to drift very slowly around the North Pole (or the NPC), by ~2.6° eastward in System III longitude. The changes between the observations taken by JunoCam are based on images of the sunlit side of the poles on PJ1, P3, PJ4 and PJ5. On the other hand, JunoCam polar images have ~90-180° overlap in sunlit longitudes between successive perijove observations in similar 53-day intervals, and can also be compared with the complete map from JIRAM at PJ4. They show that the eight CPCs are preserved throughout the entire seven-month

period, retaining their individual morphological characteristics, and showing only minor movements (Figure 2). The visible sector of the octagon rotated around the north pole as follows (positive is westward): PJ1 to PJ3: ~+2º; PJ3 to PJ4: -4 to -7.5º; PJ4 to PJ5: 0 to -3.5º. Thus, the octagon has not shown any progressive rotation about the pole in System-III longitudes. Both instruments observe small meridional displacements of individual CPCs of the same order of magnitude. For the CPCs at the South Pole, JunoCam comparisons between perijoves do suggest a progressive counter clockwise zonal rotation relative to the SPC of +1° every 53 days, as well as some wandering of individual CPCs. There are significant variations in the spacing of the CPCs around the pentagon, associated with opening and closing of a gap that is always present between two of them. Just as in the north, the cyclones have preserved their individual morphologies over the seven months of observations.

Two questions arise from these data. The first is why the pentagon and octagon drift so slowly or not at all. By Stokes' theorem, net cyclonic vorticity at the centre would imply cyclonic circulation around the periphery. The other question is why the vortices do not merge. Saturn has a single cyclonic vortex at each pole. By analysing the conditions for formation of the Saturn vortex and comparing its conditions with Jupiter ones, it was predicted that the polar circulation could have been different on Jupiter[9]. Some studies[21], applying the theory to the merger of Jupiter's white ovals in 1998-2000, have also shown that like-signed vortices merge on a fast, advective time scale of 4 months when they are no longer separated by oppositely-signed vortices in a vortex street. Mergers of the polar cyclones are possible, but they have not occurred over 7 months of observation, nor is there any evidence of new structures appearing inside the CPC polygons. Finally, on the other hand, other studies[22,23] show that polygonal vortex patterns (vortex crystals) can develop due to interaction with a background of weaker vorticity and last indefinitely in a 2D Euler flow.

Table 1: **Spin velocities of the single cyclones** calculated at the radial distance of approximately 1,500 km from their spinning centres during PJ4 by JIRAM images. There were not enough data to compute the velocity of Northern CPC#2. The numbers of the Northern CPCs go from 1 to 8 proceeding in counter clockwise and CPC#1 is the one located at 0° longitude. South Pole CPC numbering starts from the cyclone at 150° longitude and proceeds counter clockwise. Letters in parentheses identify the CPC if present in Figure 4. A quick calculation assuming the gradient wind balance, which includes Coriolis, centrifugal and pressure forces, indicates pressure gradients of the order of 5~10 Pa/km at that distance of 1500 km from the CPC centres.

North Pole				South Pole			
Cyclone CPC #	Angular velocity °/min	Tangent Velocity km/h	Full Rotation hours	Cyclone CPC #	Angular velocity °/min	Tangent Velocity km/h	Full Rotation hours
NPC	0.17	267	35.3	SPC	0.19	299	31.6
1	0.22	343	27.5	1 (H)	0.13	204	46.1
3 (D)	0.21	337	28.0	2	0.17	273	34.5
4 (E)	0.10	157	60.0	3	0.16	252	37.5
5 (F)	0.12	296	48.0	4	0.21	330	28.6
6	0.19	295	32.0	5 (G)	0.17	273	34.5
7	0.22	354	26.6				

8	0.12	296	48.0				

References

1. Porco et al., Cassini Imaging of Jupiter's Atmosphere, Satellites, and Rings, Science 299, 1541-1547, DOI: 10.1126/science.1079462 (2003).
2. Rhines P. B. Waves and turbulence on a beta-plane. Journal of Fluid Mechanics, 69(03),417-443 (1975).
3. Theiss J. Equatorward energy cascade, critical latitude, and the predominance of cyclonic vortices in geostrophic turbulence. Journal of physical oceanography. 34, 1663-1678 (2004).
4. Sayanagi, K.M., Showman, A.P., & Dowling, T.E. The Emergence of Multiple Robust Zonal Jets from Freely Evolving, Three-Dimensional Stratified Geostrophic Turbulence with Applications to Jupiter. Journal of the Atmospheric Sciences, 65(12), 3947-3962 (2008).
5. Cho, J. Y. K., & Polvani, L. M. The emergence of jets and vortices in freely evolving, shallow-water turbulence on a sphere. Physics of Fluids, 8, 1531-1552 (1996).
6. Iacono, R., M. V. Struglia, and C. Ronchi. Spontaneous formation of equatorial jets in freely decaying shallow water turbulence. Physics of Fluids 11.5, 1272-1274 (1999).
7. Showman, A. P. Numerical simulations of forced shallow-water turbulence: Effects of moist convection on the large-scale circulation of Jupiter and Saturn. Journal of the Atmospheric Sciences, 64(9), 3132-3157 (2007).
8. Scott, R. K., Polvani, L. M. Forced-dissipative shallow-water turbulence on the sphere and the atmospheric circulation of the giant planets. Journal of the Atmospheric Sciences, 64(9), 3158-3176 (2007).
9. O'Neill, M. E., Emanuel, K. A., Flierl, G. R. Polar vortex formation in giant-planet atmospheres due to most convection. Nature Geosci. 8, 523-526. doi:10.1058/ngeo2459 (2015).
10. Bolton S.J. et al. Jupiter's interior and deep atmosphere: The initial pole-to-pole passes with the Juno spacecraft. Science 356, 821-825, doi: 10.1126/science.aal2108 (2017).
11. Connerney J.E.P. et al. Jupiter's Magnetosphere and Aurorae Observed by the Juno Spacecraft During its First Polar Orbits. Science 356, 826-832, http://dx.doi.org/10.1126/science.aam5928 (2017).
12. Grassi D. et al. Preliminary results on the composition of Jupiter's troposphere in Hot Spot regions from the JIRAM/Juno instrument. Geophysical Research Letters, Volume 44, doi: 10.1002/2017GL072841 (2017).
13. Sindoni G. et al. Characterization of the white ovals on Jupiter's southern hemisphere using the first data by the Juno/JIRAM instrument. Geophysical Research Letters, Volume 44, doi: 10.1002/2017GL072940 (2017).

14. Orton, G. S. et al. , The first close-up images of Jupiter's polar regions: results from the Juno mission JunoCam instrument. Geophys. Res. Lett. 44, doi:10.1002/2016GL072443 (2017). 6
15. Orton, G. S. et al. Multiple views of Jupiter from Juno and Earth-based observations. Geophys. Res. Lett. 44, doi: 10.1002/2017GL073019 (2017).
16. Adriani A. et al. IRAM, the Jovian Infrared Auroral Mapper. Space Sci. Rev., DOI 10.1007/s11214-014-0094-y (2014).
17. Adriani A. et al. Juno's Earth flyby: the Jovian infrared Auroral Mapper preliminary results, Astrophys Space Sci, DOI 10.1007/s10509-016-2842-9 (2016).
18. Hansen, C.J. et al. Junocam: Juno's Outreach Camera, Space Sci. Rev. doi 10.1007/s11214-014-0079-x (2014).
19. Theiss, J. A generalized Rhines effect and storms on Jupiter. *Geophysical Research Letters* 33, 8 (2006).
20. LeBeau and Dowling. EPIC Simulations of Time-Dependent, Three-Dimensional Vorticeswith Application to Neptune's Great Dark Spot. Icarus 132, 239-265 (1998).
21. Youssef, A., P. S. Marcus. The dynamics of jovian white ovals from formation to merger. Icarus 162, 74-93 (2003).
22. Fine K.S., A.C. Cass, W. G. Flynn, and C. F. Driscoll. Relaxation of 2D Turbulence to Vortex Crystals. Phys. Res. Let. 75, 3277-3280 (1995).
23. Schecter D.A., D.H.E. Dubin, K.S. Fine, and C.F. Driscoll. Vortex crystals from 2D Euler flow: Experiment and simulation. Phy. Of Fluids 11, 905-914 (1999).

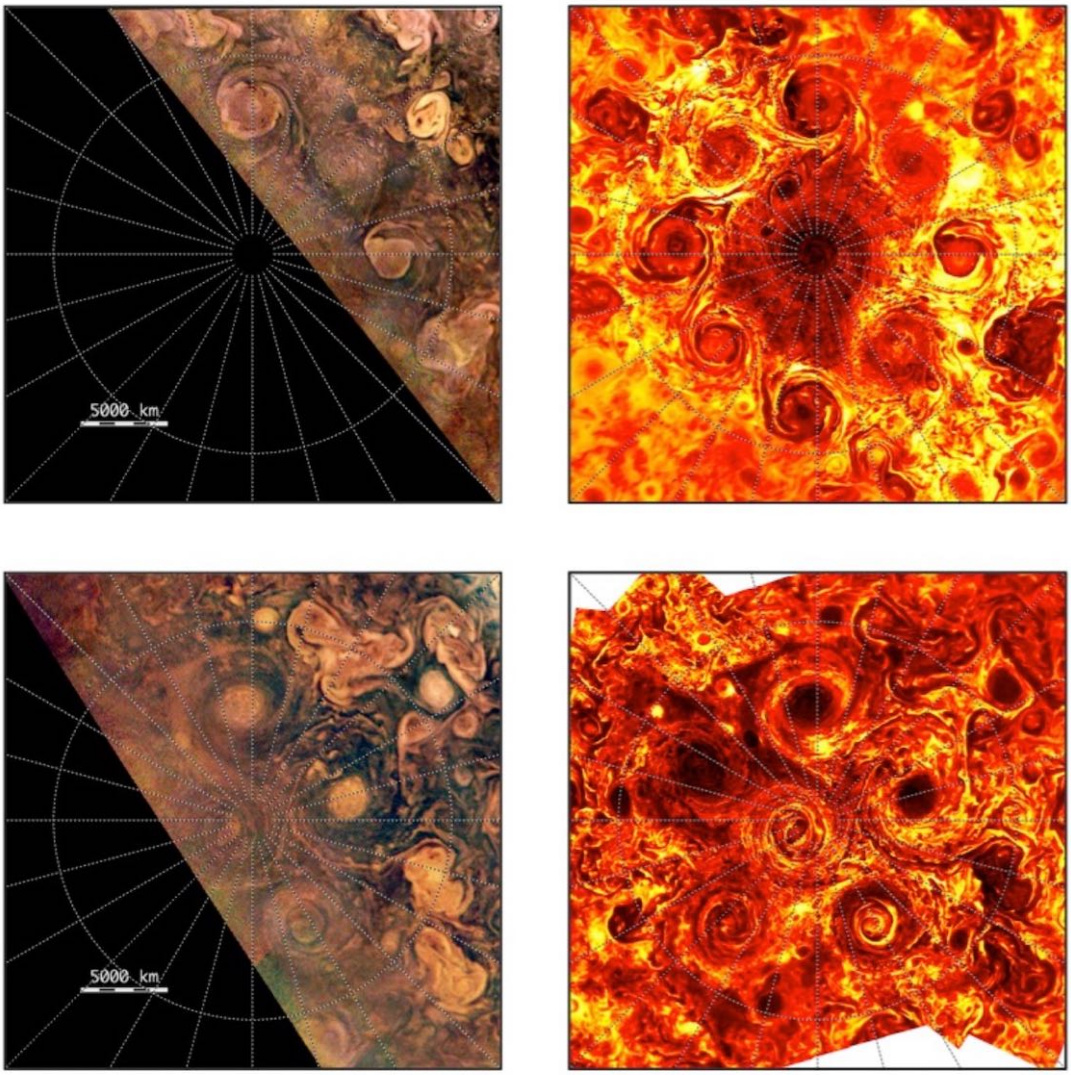

Figure 1 | Jupiter Poles as they appear at visible and infrared wavelengths. Projected maps of the North pole (top) and South pole (bottom) regions from the JIRAM 5-μm M-filter observations (right-hand panels) and JunoCam color-composite images (left-hand panels) during PJ4 on 2 February 2017. Latitude circle = 80°N or S (planetocentric). Meridians are drawn every 15° of longitude, and 0°W in System III is positioned on the right centre of the images. By operating at thermal-infrared wavelengths, JIRAM observes the atmospheric structures regardless of solar illumination, whereas JunoCam's optical images are restricted to only the illuminated hemisphere, which is why only part of the JunoCam map for the north pole in Figure 1 is present. JIRAM radiance, ranging from 0.02 (dark red) to 0.8 W m^{-2} sr^{-1} (white) is corrected with respect to the emission angle; the radiance scale is logarithmic. The JunoCam images are corrected with respect to solar illumination angle, as discussed by Orton et al.[5] and the colours of the maps were stretched and balanced to enhance atmospheric features. Cyclonic features can be seen clustered around each pole with regular circular shapes, some with spiral arms. For the South polar region, we note that there is a wider longitude separation (a "gap") between the CPCs near 180°W (centre left side) than between the other cyclones. Two smaller cold features can be seen to the upper left of the NPC, which are anticyclonic vortices.

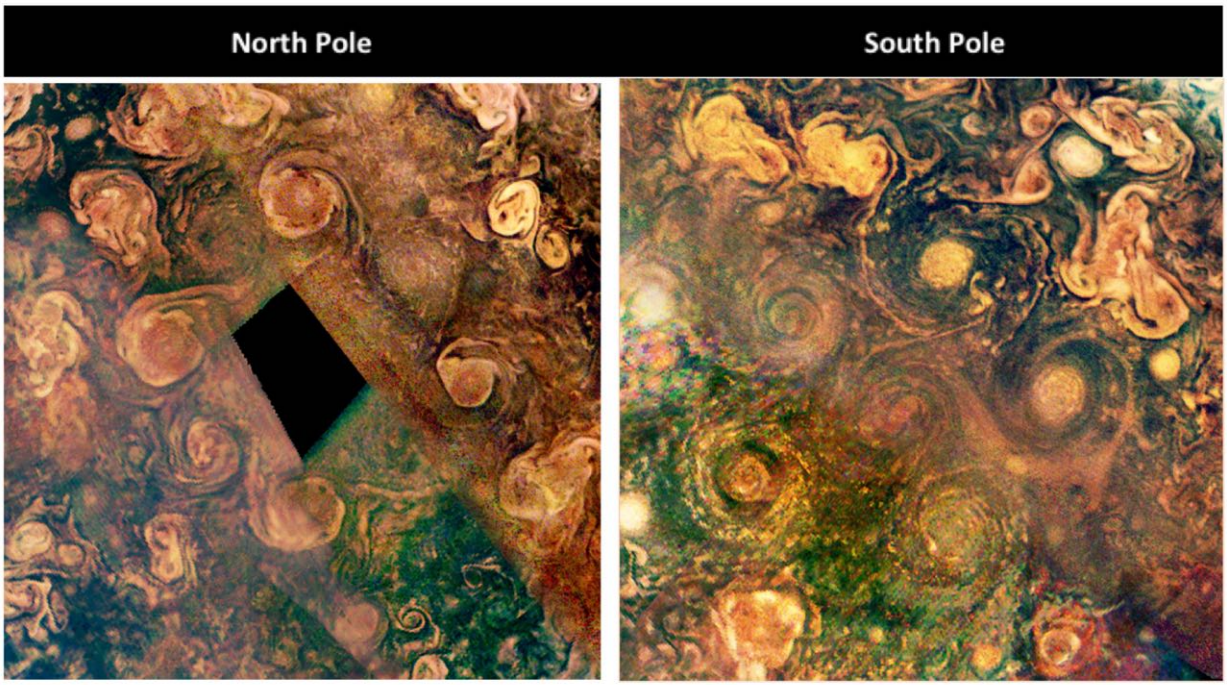

Figure 2. | The Poles observed by JunoCam during the first four passes at Jupiter. Composite of the polar regions observed by JunoCam not only at PJ4 but also at complementary longitudes, acquired in PJ1, PJ3 and PJ5 for regions not illuminated by sunlight in PJ4. The PJ4 projection has been preserved as in the left-hand panels in Fig. 1; the remainder of the unfilled space covered by a composite of image from the other perijoves. The remaining regions that are dark in Figure 1 are a smooth composite of JunoCam images taken on PJ1, PJ3 and PJ5. The dark region in the centre of the North polar region is the result of those latitudes being not illuminated. Elsewhere on Jupiter, cyclonic circulations assume a variety of forms, especially at high latitudes, but none are simple spirals with circular outlines, except for very small ones. We note that, although they were imaged 53-106 days (1-2 Juno orbits) from the PJ4 observations, the positions and even the gross morphologies of the CPCs imaged during those orbits are not very different from their overall morphology in the PJ4 JIRAM map. The JunoCam map colours were chosen to enhance atmospheric features.

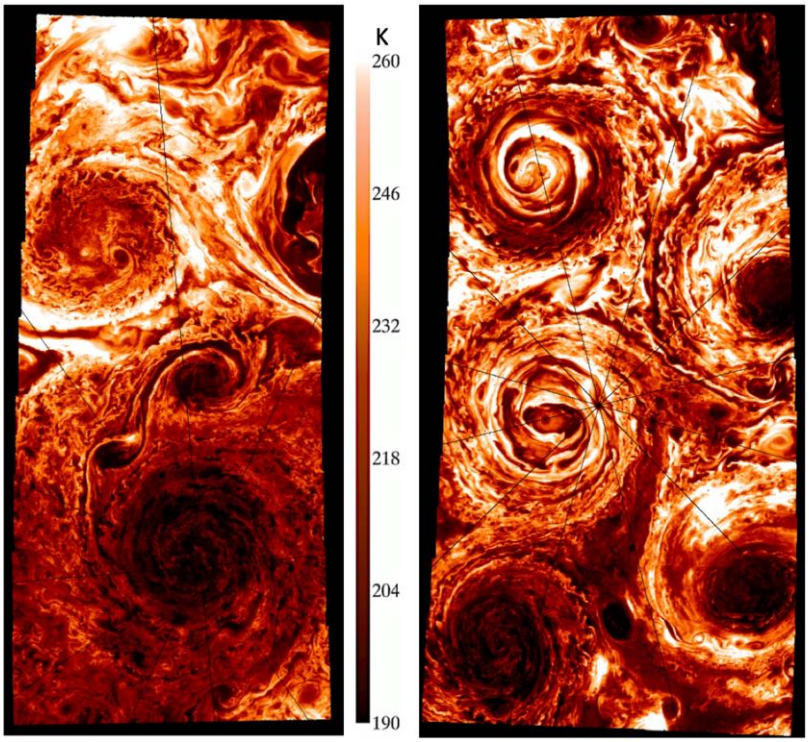

Figure 3. | High resolution view of the polar vortices. Left panel: North Pole as seen in the 5-μm spectral region (JIRAM M-filter) at an average spatial resolution of 18 km/pixel. Right panel: South Pole at an average spatial resolution of 25 km/pixel in the same filter. These maps represent the highest available spatial resolution of JIRAM images on PJ4. The red color scale from black to white is associated to the apparent brightness temperature of the pictured areas, covering 190 – 260 K. Some cyclones look more clearly structured with alternating cold (cloudier) and warm (clearer) banding as a function of radius. It also clearly depicts the mesoscale dynamics over Jupiter's polar regions showing a quite chaotic environment with many wavy structures and smaller anticyclones and cyclones developing among the largest ones. Such small anticyclonic eddies can be seen between some of the cyclones, especially around the NPC, where the largest of them measures about 1200 km in diameter. There is a great structural difference between the NPC, which is dominated by a very small-scale cloud structure, and the SPC, which is characterized by a quasi-laminar behaviour. The SPC has a diameter of about 5,800 km and its centre is very peculiar, presenting an elongated "eye-shape" instead of the circular structure characterizing the center of all the other cyclones.

Acknowledgments

The JIRAM project is founded by the Italian Space Agency (ASI). In particular this work has been developed under the ASI-INAF agreement n. 2016-23-H.0. The JunoCam instrument and its operations are funded by the National Aeronautics and Space Administration. A portion of this work was supported by NASA funds to the Jet Propulsion Laboratory, California Institute of Technology, and to the Southwest Research Institute. API was supported by NASA funds to the Juno project and by NSF grant number 1411952.

Author Contributions

AA and CH are the Juno mission instrument leads for the JIRAM and JunoCam instruments, respectively, and they planned and implemented the observations discussed in this paper. SJB and JEPC are respectively the principal and the deputy responsible for the Juno mission. AA, AMu, GO, JR, AI and FT were responsible for writing substantial parts of the paper. MEO gave important suggestions for the interpretation of the cyclonic structure. AMu, FA, MLM and DG were responsible for reduction and measurement of the JIRAM data and their rendering into graphical formats. GE, TM, GO and JR were responsible for the same tasks for JunoCam data. FT and FF are responsible for the geometric calibration of the JIRAM data. GF, GS, BMD and SS are responsible for the JIRAM data radiance calibrations. AC, RN and RS are responsible for the JIRAM ground segment. SA, JIL, AMi, DT, GP and DT have supervised the work. CP, AO and MA are responsible for the JIRAM project from the Italian Space Agency side.

Competing Financial Interests: The authors declare no competing financial interests.

METHODS

The Jovian InfraRed Auroral Mapper

The Jovian InfraRed Auroral Mapper (JIRAM) is composed of an imager and a spectrometer that share the same telescope[7,8]. The imager focal plane is equipped to observe the planet through a bandpass filter centered at 4.78 μm with a 480-nm bandwidth (M-band) and a bandpass filter centered at 3.45 μm with a 290 nm bandwidth (L-band). The spectrometer's slit is optically co-located with the imager's field of view (FOV) and its spectral range covers the 2-5 μm interval in 336 spectral bins (bands) resulting in a spectral sampling of 8.9 nm/band across the full spectral range. The instrument design allows acquisition of simultaneous imager and spectrometer observations: in this study, we used the data from the M band filter, which covers a FOV of about 1.75° by 6° with 128 by 432 pixels. The instantaneous field of view (IFOV) is 240 μrad (see Adriani et al.[8] for instrumental details).

At the time of the observations, the Juno spacecraft was spinning almost perpendicular to the orbital plane. For each spin, JIRAM takes two images: one to the target (nadir direction), and one to the anti-nadir direction, to evaluate the background, which is removed on-board. JIRAM is also equipped with a de-spinning mirror that compensates for the spacecraft rotation and enables it to keep the target image in the field of view during the data acquisition. The de-spinning mirror may also be activated at different times with respect to the nadir direction, allowing a scan of the planet in the spacecraft's spinning plane. No pointing outside of the spinning plane is permitted.

The data shown in this paper (integrated radiance from 4.5 to 5 μm) have been taken with 12 ms of integration time, resulting in a noise-equivalent radiance lower than 5 10-5 W sr-1 m-2. Table 1 shows exact times of observations (start time, stop time and number of observations in that sequence/scan). JIRAM observed both poles with high image quality and spatial resolution during the perijove passes 4 (PJ4) and 5 (PJ5). Polar coverage during PJ4 was complete for regions within 30° latitude of both poles with a spatial resolution varying between 12 and 96 km/pixel for North Pole and between 21 and 62 km/pixel for South Pole. JIRAM coverage of the poles during PJ5 was incomplete, limited by JIRAM's field of view (FOV) and Juno's spin axis orientation during perijove.

While data of PJ4-North Pole has a complete coverage with good emission angle (i.e. close to 90°), to cover the other 3 cases we use also radiance emitted at lower angles. Such radiance is partially depleted because the absorption due to cold clouds occurs over a longer path. A simple correction was applied, mainly with the purpose of better identifying the same features at both PJ4 and PJ5. Since during PJ4 JIRAM observed the same regions of the north pole at different emission angles, such data were used to compile a look-up table that, given the measured radiance and the emission angle, returns the estimated value of radiance at 90°.

Data are jovian-located and then re-projected in System-III planetocentric geographical coordinates, using a polar orthographic projection. Geometric information was obtained by using ad hoc algorithms based on the NAIF-SPICE tool[24] for each image. JIRAM raw data are calibrated in units of radiance ($Wm^{-2}sr^{-1}$) as described by Adriani et al.[7,8]. The responsivity used in this study has been revised to a flat value of 2 10^6 DN / (W sr^{-1} m^{-2}) by using the cruise calibration campaign data, performed by using Aldebaran as a reference target.

Finally, the diameters of the cyclones are calculated on the JIRAM infrared images, defining the outer border of the cyclone where the smaller, anticyclonic structures form and planetocentric coordinates are used throughout this report.

Images from JIRAM have been processed by using Matlab (Figure 1 and Extended Data Figure 1) and ENVI-IDL (Figure 3).

Processing of consecutive images allows for animations revealing motion, as well as for quantitative analysis of cloud velocities. JIRAM data in EXTENDED DATA Table 1 have been arranged in animations that show the movement of single vortices during PJ4 observations. Each sequence/scan has been composed in a mosaic, and then each mosaic became a frame of the video. We provide 9 videos for the North Pole (8 CPC plus the PC); each video is made of 11 images. We also provide 6 videos for the South Pole (5 CPC plus the PC); each video is made of 6 images.

JunoCam

JunoCam is a pushframe visible camera designed to acquire images through broadband red, green and blue filters mounted directly on a CCD detector, with an 889-nm methane absorption band filter acquiring an image on a separate rotation typically 30 seconds later. JunoCam is rigidly mounted on the spinning spacecraft. That way, it can take a full panorama within about 30 seconds consisting of up to 82 narrow exposures. Usually, it takes partial panoramas of the target of interest. The camera has a horizontal field of view of about 58°, and Kodak KAI-2020 CCD sensor with four filter stripes, a red, a green, a blue and a narrow-band 890-nm infrared filter attached on the 1600x1200 light-sensitive pixels. For each of the four filters, there is an corresponding readout region of 1600x128 pixels which can be transferred into the resulting raw image. This transfer isn't immediate, but the 12-bit data number of each pixel is encoded as an 8-bit value, and tiles of 16x16 pixels are compressed either lossy or lossless. Usually, the encoding of the 12-bit data as an 8-bit value is nonlinear according to a companding function. Motion blur is mostly avoided by a technique called time delay integration (TDI). In RGB mode, for each exposure, three of the four readout regions are added as stripes to the raw image. Full details about the instrument and its operation are available in Hansen et al.[9].
JunoCam observed the same polar regions as JIRAM on PJ4 and PJ5 – as well as complementary longitudinal regions on PJ1 and PJ3 – but as a visible imager, it acquires images in reflected light. A complete polar view must be pieced together from the unshadowed portions of images collected during multiple perijove passages.

Observations were made in both North and South polar regions in perijoves PJ1, PJ3, PJ4, PJ5. Polar imaging in PJ5 was scheduled over extended periods of time in order to cover more longitudes as the planet rotates through daylight, which enabled time-lapse measurments that include measurements of rotation of the CPCs.

With an approximate geometrical camera model, including its pointing for each exposure, the appropriate 3D vector was calculated for each pixel in a given reference frame, e.g. J2000. Position and pointing information are inferred from SPICE data[21], with some manual adjustment. Jupiter is modeled as a MacLaurin spheroid on Jupiter's 1-bar level. A planetocentric coordinate system assigns a 3D position to each longitude/latitude pair. The 3D vector, pointing from Juno to the 3D position, completes the connection of each longitude / latitude pair to color

information. With this method, each raw JunoCam image of Jupiter is reduced to an approximately geometrically calibrated polar-map projection.

Because Jupiter is rotating and Juno is moving rapidly, the illumination for each JunoCam image changes rapidly. Comparison of images requires approximate normalization of the images. For now, this is achieved in a heuristic way, essentially stretching contrast over regions of approximately similar solar incidence angles, subtracting the mean brightness for these bins, and accounting for changing light scattering of a presumed haze layer as a function of emission angle, which can be obtained for sufficiently small crops by high-pass filtering. For the JunoCam maps shown in Figs. 1 and 2, this correction was made down to a maximum solar-illumination angle of 66°, above which the signal-to-noise ratio drops below 3 per pixel. Further nonlinear brightness stretching and saturation enhancement brings out detail.

Time sequences of 2- to 3-frames of polar images were made on all perijoves to track cloud motions. After PJ1, it was clear that the limited time sequence on that orbit verified the visible impression that the features surrounding the poles whose "arms" implied cyclonic motion really were cyclones. A special effort was made in PJ5 to create longer sequences of time-lapse images that would illustrate subtler motions of the polar features by imaging over a longer time interval. The sequences given below represent three of the best of those animations.

- A sequence of images from the north pole is available in the file: jnc_pj05_N_089_to_105_blend4_enh.gif.
- A sequence of images from the south pole is available in the file: jnc_pj05_polarS_60px_lin_inerpolated_21frames_1200x1200.gif.
- A close-up version of that south polar sequence is available in the file: jnc_pj05_south_polar_animation_111_to_121_8frames_20fps_1200px.gif.

History and terminology of cyclone clusters

The term "ditetragonal" has been introduced in the context of crystallography, since it is one of the ten two-dimensional crystallographic point groups, see:
"International Tables for Crystallography", Volume A, Space group symmetry, edited by Th. Hahn, Fifth edition 2002, Corrected Reprint 2005.
http://www.fisica.unam.mx/laboratorios/lmna/didactico/ITC-Vol.A%20(2005)(ISBN%200792365909).pdf
(more officially: http://onlinelibrary.wiley.com/book/10.1107/97809553602060000001), p. 768, Table 10.1.2.1. 'The ten two-dimensional crystallographic point groups.'

In the non-euclidean geometry of the curved polar region a two-dimensional pentagonal rather than a hexagonal pattern would be conceivable, similar to the surface of a pentagon-dodecahedron. (*ibid.,* p. 786, Table 10.1.2.2, 'The 32 three-dimensional crystallographic point groups (cont.), Cubic system')

But since the size of the vortices does not fit exactly to the geometry of a pentagon-dodecahedron, we could get an unstable structure switching between a hexagon and pentagon, or an oscillating pentagon for vortices of similar size.

In addition to the references to 'vortex crystals' cited in the main paper, similar vortex patterns occur also in rotating superfluid helium-II for quantum-mechanical reasons:
https://www.researchgate.net/figure/222541566_fig4_Figure-5-Vortex-patterns-in-a-rotated-sample-of-superfluid-Helium-with-1-11
Theoretical predictions of such quantized vortices reach back to Onsager (1949) and Feynman (1955), although Landau introduced rotons in 1941.
R.P.Feynman (1995) Progress in Low Temperature Physics, Vol. 1, pp. 17-53: Chapter II: 'Application of Quantum Mechanics to Liquid Helium'
https://doi.org/10.1016/S0079-6417(08)60077-3
http://www.sciencedirect.com/science/article/pii/S0079641708600773
The first experimental observations were in 1979:
E.J. Yarmchuk, M.J.V. Gordon, and R.E. Packard, 'Observation of Stationary Vortex Arrays in Rotating Superfluid Helium', Phys. Rev. Lett. 43, 214 (1979).
https://journals.aps.org/prl/abstract/10.1103/PhysRevLett.43.214

Data availability. The data used for this study will be available once the proprietary period ends from the NASA's Planetary Data System at https://pds.jpl.nasa.gov/tools/data-search/.

Methods reference

24. Acton, C.H. Ancillary data services of NASA's navigation and ancillary information facility. Planet. Space. Sci. 44, 65-70 (1996).

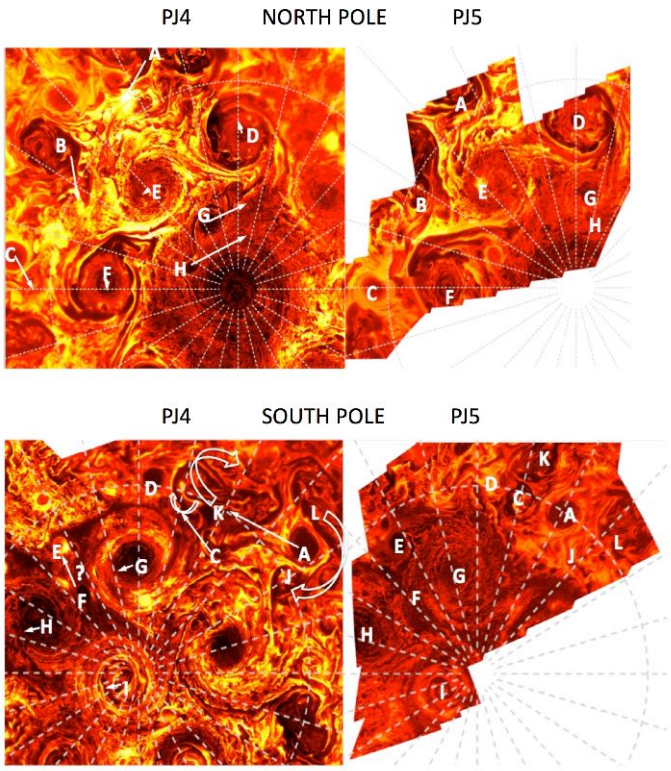

EXTENDED DATA Figure 1. Comparison of the Poles cyclonic structures between PJ4 and PJ5. Here is the comparison between JIRAM 5-μm data acquired during PJ4 and PJ5. The letters possibly identify recurrent structures and arrows show the suggested displacements that occurred in the 53-day interval between these two perijoves. The radiance scale is the same as in Figure 1.

The region surrounding the geographic North Pole is not sunlit, then there are no JunoCam observations of the NPC. On the other hand, although North Pole was detected by JIRAM on PJ4, we were unable to determine whether or not it maintains a stable position over the geographic North Pole because of insufficient coverage of the NPC during PJ5. However, the cyclonic structures A, B and C move northeast migrating from the lower latitudes. The G and H internal structures, located between the NPC and the CPCs, are anticyclones and move westward in that narrow corridor between 85.5°N and 87°N to their new location observed during PJ5 between vortex D and the NPC.

On the contrary, JIRAM was able to observe the SPC both in PJ4 and PJ5. In fact, along with the cyclones G and H shown, the SPC moves northward, increasing its distance with respect to the geographic South Pole of 1.5° between PJ4 and PJ5. On the other hand, JunoCam was able to observe the SPC at all perijoves, and found that it was always displaced from the South Pole in approximately the same direction (towards a System III longitude of ~219±21°), with its central latitude varying from 88.0ºS at PJ1 up to 89.0ºS at PJ4, and down to 88.4ºS at PJ5. It remains to be seen whether this is a cyclic oscillation. The five CPCs remain at almost constant radial distances from the center of the SPC (and thus not the geographic South Pole), so the whole pentagon drifts in latitude. Anticyclone A appears to move as much as ~1° south and ~24° east. It is forced and surrounded by the two cyclonic structures that consolidate themselves between PJ4 and PJ5 from the origins L, J, C and K. Finally, the anticyclone D disappears while F is expelled from its position and possibly moves to new position E.

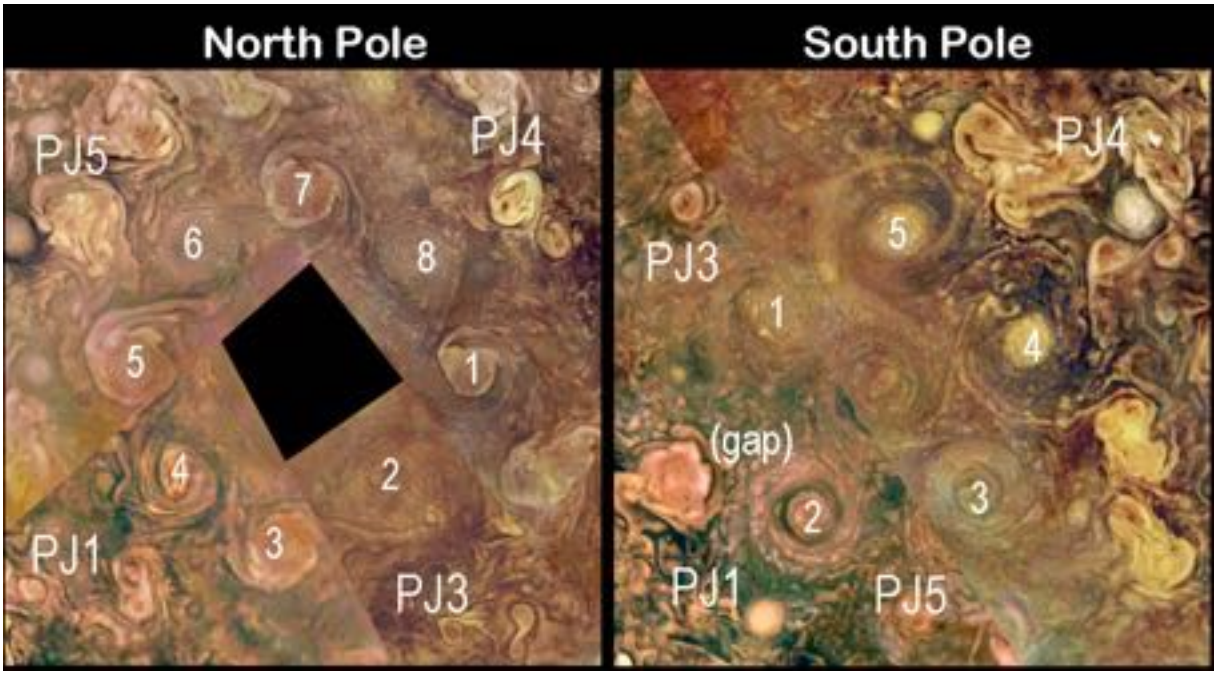

EXTENDED DATA Figure 2. **Annotated version of Figure 2 of the main text.** The composite components from each perijove that were used to create the figure are noted. Each corresponds to the polar image taken at a time that minimized the emission angle over most of the pole, as detailed in Table 2. The PJ4 component is identical to its contribution in Figure 1, with contributions from the other perijoves, separated by approximately 90° in longitude, as noted. The northern CPCs forming the inner square (actually a rhombus) of the ditetragonal pattern are labelled by odd numbers and those forming the outer square by even numbers. The southern CPCs forming a quasi-pentagonal shape are numbered sequentially, with the largest spacing between CPCs labelled 1 and 5, indicated by the "(gap") label. Despite the time differences between JIRAM images acquired on PJ4, shown broadly in the right-hand panels of Figure 1, and JunoCam images in PJ1, PJ3 and PJ5 – time differences of 53 to 106 terrestrial days, the positions of the CPCs are remarkably consistent in the System III longitude.

North Pole, 4th perijove, 2017-02-02		
Start UTC	Stop UTC	observations
08:10:24	08:15:59	12(1)
08:18:31	08:24:07	12(1)
08:26:08	08:31:44	12(1)
08:34:16	08:39:51	12(1)
08:42:23	08:47:59	12(1)
08:50:31	08:56:06	12(1)
08:58:08	09:03:43	12(1)
09:06:15	09:11:51	12(1)
09:14:23	09:19:58	12(1)
09:22:30	09:28:06	12(1)
09:30:07	09:35:43	12(1)
09:38:15	09:43:50	12(1)
09:46:22	09:51:58	12(1)
11:00:00	11:05:35	12(2)
11:08:07	11:13:43	12(2)
11:16:14	11:21:50	12(2)
11:24:22	11:29:57	12(2)
11:31:59	11:37:34	12(2)
11:40:06	11:45:41	12(2)
11:48:13	11:53:48	12(2)
11:56:20	12:01:55	12(2)
12:04:26	12:10:02	12(2)
12:12:02	12:17:38	12(2)
12:20:07	12:25:44	12(2)

South Pole, 4th perijove, 2017-02-02		
Start UTC	Stop UTC	observations
13:58:59	14:08:08	19
14:18:46	14:27:55	19
14:39:04	14:48:13	19
14:58:53	15:08:02	19
15:18:41	15:27:50	19
15:39:00	15:48:09	19

North Pole, 5th perijove, 2017-03-27		
Start UTC	Stop UTC	observations
08:14:20	08:16:20	5
08:18:49	08:24:19	12
08:26:48	08:30:48	9
08:33:17	08:33:47	2

South Pole, 5th perijove, 2017-03-27		
Start UTC	Stop UTC	observations
09:17:54	09:18:54	3
09:21:23	09:24:24	7
09:26:53	09:29:53	7
09:32:23	09:33:53	4

EXTENDED DATA Table 1. JIRAM Start time, stop time and number of observations for the different datasets used for this study. (1) Approach phase, low resolution; used only to fill small gaps in Figure 1; (2) minimum emission angle, high resolution, used to make most of the mosaic in Figure 1.

Pole	Perijove	Date	Time (UTC)	File Name
North	1	2016-08-27	11:57:40-11:57:49	JNCE_2016240_00C06160_V02_553
South	1	2016-08-27	11:59:12-11:59:21	JNCE_2016240_00C06186_V02_579
North	3	2016-12-11	16:13:45-16:13:54	JNCE_2016346_03C00099_V02_588
South	3	2016-12-11	18:10:49-18:10:56	JNCE_2016346_03C00126_V02_615
North	4	2017-02-02	12:08:22-12:08:32	JNCE_2017033_04C00097_V01_624
South	4	2017-02-02	14:06:29-14:06:38	JNCE_2017033_04C00109_V01_636
North	5	2017-05-19	08:04:43-08:04:52	JNCE_2017086_05C00102_V01_890
South	5	2017-05-19	10:01:48-10:01:55	JNCE_2017086_05C00118_V01_901

EXTENDED DATA Table 2. Details of the JunoCam observations used in Figures 1, 2 and in EXTENDED DATA Figure 2.